Frontiers in Bioscience Landmark

Front. Biosci. (Landmark Ed) **2026**; 31(4): 49495
https://doi.org/10.31083/FBL49495

Original Research

ADAM8 Deficiency in Macrophages Alleviates Vascular Calcification in Chronic Kidney Disease

Rong Dong[1,2,3,4], Zhenjun Ji[1,2], Mi Wang[1,2], Zaixiao Tao[1,2], Xinxin Li[1,2], Rui Zhang[1,2], Junwei Xu[1,2,5,*], Genshan Ma[1,2,*]

[1]Department of Cardiology, Zhongda Hospital, 210009 Nanjing, Jiangsu, China
[2]School of Medicine, Southeast University, 210009 Nanjing, Jiangsu, China
[3]Department of Cardiology, Yancheng No. 1 People's Hospital, Affiliated Hospital of Medical School, Nanjing University, 224000 Yancheng, Jiangsu, China
[4]Department of Cardiology, The First people's Hospital of Yancheng, 224000 Yancheng, Jiangsu, China
[5]Department of Cardiology, Nanjing Chest Hospital, Affiliated Nanjing Brain Hospital, Nanjing Medical University, 210029 Nanjing, Jiangsu, China
*Correspondence: christxjw@163.com (Junwei Xu); magenshan@hotmail.com (Genshan Ma)
Academic Editor: Paramjit S. Tappia
Submitted: 27 December 2025 Revised: 16 March 2026 Accepted: 24 March 2026 Published: 22 April 2026

Abstract

Background: Vascular calcification (VC) is an inflammatory disease driven by aberrant cellular processes in which macrophages play an important role. The A disintegrin and metalloproteinase 8 (ADAM8) protein is an important regulatory factor in macrophages and contributes to the development of inflammatory diseases. However, the relationship between ADAM8 and VC remains unknown. Thus, this study aimed to investigate the role of macrophage ADAM8 in VC. **Methods**: Plasma ADAM8 levels were compared between patients with and without aortic calcification. Immunofluorescence staining of human aortic tissue samples was performed to assess differences in ADAM8 expression between calcified and non-calcified tissues. Macrophage-specific *Adam8* knockout mice (*Adam8*$^{flox/flox,\ Lyz2\text{-}Cre}$; KO) and the corresponding control mice (*Adam8*$^{flox/flox}$; Flox) were generated using CRISPR/Cas9 technology. Additionally, the adeno-associated virus AAV6-F4/80-*Adam8* was employed to achieve macrophage-specific overexpression. The relationship between macrophage ADAM8 and VC was studied in a VC mouse model of chronic kidney disease (CKD) by comparing VC severity between groups. **Results**: Plasma ADAM8 levels were elevated in patients with aortic calcification. Immunofluorescence staining of human aortic samples suggested that VC was associated with ADAM8-positive macrophage infiltration and ADAM8 released by macrophages. In mice, macrophage-specific *Adam8* knockout attenuated the development of CKD-associated VC, whereas macrophage-specific ADAM8 overexpression reversed the VC phenotype. **Conclusion**: ADAM8 levels are elevated in patients with aortic calcification and are associated with macrophage infiltration into vascular tissue and ADAM8 release, leading to increased VC. These findings identify ADAM8 as a promising novel therapeutic target for preventing VC.

Keywords: A disintegrin and metalloproteinase 8 (ADAM8); macrophage; vascular calcification; inflammation; chronic kidney disease (CKD)

1. Introduction

Vascular calcification (VC) is characterized by the deposition of calcium phosphate on arterial walls and is an independent predictor of adverse cardiovascular events [1]. VC is commonly associated with aging [2], chronic kidney disease (CKD) [3], atherosclerosis [4], hypertension [5], and certain hereditary diseases. Due to population aging and other risk factors, the incidence of VC has increased in recent decades, constituting a threat to global public health. VC occurs insidiously, as it is clinically silent. It has a prolonged course, yet its progressive development is often overlooked, which can result in hemodynamic impairment associated with chronic ischemia in various organs. Ultimately, this can lead to adverse outcomes such as acute myocardial infarction, stroke, and peripheral arterial occlusion [6]. Due to the lack of effective preventative measures, most current treatments for VC, which are invasive and downstream modalities, target calcified vascular tissue. Although revascularization techniques can improve the survival rate of some vascular stenoses or occlusive diseases, the incidence of surgical complications and poor prognosis due to calcified vessels means that treating VC remains a formidable challenge.

Moving beyond theories of passive calcium phosphate deposition, VC is now understood to be an active, cell-driven process. This process is tightly controlled by various inducers and inhibitors, sharing fundamental cellular mechanisms, regulatory pathways, and structural characteristics with bone formation [7–11]. A key step in the development of VC is the osteogenic differentiation of vascular smooth muscle cells (VSMCs) [12]. Although the drivers and mechanisms underpinning the development of VC vary in different conditions, the pathological features of phenotypic transition are essentially the same. Fundamentally,

these phenotypic shifts involve the downregulation of contractile markers, including smooth muscle protein 22-alpha (SM22α) and alpha-smooth muscle actin (α-SMA), as well as the upregulation of osteogenic markers such as Runt-related transcription factor 2 (Runx2), bone morphogenetic protein 2 (BMP2), and alkaline phosphatase (ALP). Emerging evidence highlights the involvement of diverse molecular pathways and mediators in modulating VSMC phenotypic switching, including microRNAs [13], inflammatory vesicles, autophagy [14], ferroptosis [15,16], mitochondrial stress [17], and endoplasmic reticulum stress [18]. The regulatory mechanisms underlying VC have become a hot topic in current research. Elucidating these mechanisms is critical for advancing VC clinical prevention and management.

Robust evidence suggests that VC is a chronic, sterile inflammatory disease. During aging or CKD, inflammation can lead to the uptake of inorganic phosphate, which promotes the osteogenic differentiation of VSMCs. Therefore, inhibiting this inflammatory response is a key means of antagonizing VC. Furthermore, macrophage infiltration is one of the key steps in VC development. Macrophages are recognized to play a dynamic and multifaceted role throughout the course of VC, including initiation, progression, and potential regression [19]. Macrophages can be secondarily recruited to inflammation or microcalcification, which, in turn, induces the release of inflammatory factors, the expression of osteogenic genes, or the formation of apoptotic vesicles. On the one hand, this can continue to drive macrophage recruitment. However, on the other hand, some inflammatory mediators can further induce the osteogenic differentiation of VSMCs. Therefore, an in-depth study of the characteristics of infiltrating macrophages at the onset of VC and the potentially targetable upstream procalcification mediators is essential for the clinical management of VC.

A disintegrin and metalloprotease 8 (ADAM8), also known as MS2 or CD156, is a member of the ADAM protein family. *Adam8* was initially identified through cloning mouse macrophage cDNA from a library. The gene is preferentially expressed in lymphoid tissues, immune cells, and tumor cells. Structurally, ADAM8 contains the characteristic domains shared by the ADAM protein family: a prodomain (Pro), a metalloproteinase (MP) domain, a disintegrin (DIS) domain, a cysteine-rich domain (Cys), an epidermal growth factor (EGF)-like domain, a transmembrane domain (TM), and a cytoplasmic domain (CD) [20]. ADAM8 possesses protein hydrolytic activity, which is mainly responsible for the cleavage of cell membrane proteins. It is critically involved in diverse physiological and pathological processes, such as cell adhesion, differentiation, fertilization, inflammation, and tumorigenesis.

Evidence from cardiovascular disease studies suggests that plasma ADAM8 levels correlate with the severity of atherosclerosis [21]. Evidence also suggests that ADAM8 enhances osteoclast formation both *in vivo* and *ex vivo* and that it mediates bone resorption during inflammatory processes [22,23]. A strong association between osteoporosis and VC has been widely reported, and the role of ADAM8 in both inflammation and bone homeostasis suggests that it may also be involved in the pathogenesis of VC. However, the relationship between ADAM8 and VC has not been described.

Thus, the aim of this study was to investigate the relationship between macrophage ADAM8 and VC. We found that VC was associated with the macrophage infiltration of vascular tissues and the release of ADAM8. Macrophage ADAM8 in CKD-background mice promoted VC through inflammatory mechanisms, whereas the knockout of macrophage Adam8 attenuated VC in the CKD background, providing a rationale for targeted interventions against VC.

2. Materials and Methods

2.1 Patients

Eighty-five CKD patients and 44 controls were enrolled from the Cardiology Department of our hospital from July 2023 to January 2024 for the aortic calcification study. This study complied with the Declaration of Helsinki and was approved by the Ethics Committee of Southeast University-affiliated Zhongda Hospital (Number: 2023ZDSYLL298-P01). Blood was collected from the patients along with basic clinical data (**Supplementary Table 1**). The inclusion criteria were: (1) Willing participants and signing the informed consent form. (2) Individuals aged 18 years or older, excluding pregnant women. (3) Case group: patients with stage III–IV CKD; control group: individuals with normal renal function, no history of hematuria, proteinuria, or CKD, or patients with stage I CKD. The exclusion criteria were: (1) Individuals with a history of ischemic stroke within the past week, intracranial or gastrointestinal hemorrhage within the last 6 months, or major surgery within the previous 30 days. (2) Those with severe respiratory conditions, including but not limited to chronic obstructive pulmonary disease (COPD) or asthma. (3) Severe liver disease (hepatic insufficiency), with aspartate aminotransferase/alanine aminotransferase (AST/ALT) levels exceeding three times the upper limit of normal due to non-cardiac causes, or history of cirrhosis. (4) Severe infectious diseases, or patients with severe dyspnea due to conditions such as pneumonia or COPD. (5) The presence of other severe comorbid conditions that limit life expectancy to less than 6 months. (6) Cardiac conduction disorders, including sick sinus syndrome, advanced atrioventricular block, or bradycardia-induced syncope. (7) Pregnant or lactating women. (8) Participants deemed by the investigator to be otherwise unsuitable for the study.

Eight patients who had undergone aortic replacement were enrolled in this study from the cardiothoracic surgery department of Zhongda Hospital from May 2024 to July

2024 and were included in the immunofluorescence imaging of human aortic tissues. This study complied with the principles of the Declaration of Helsinki and was approved by the Ethics Committee of Zhongda Hospital, affiliated with Southeast University (Number: 2024ZDSYLL150-P01). Aortic tissues were collected from the patients. The inclusion criteria were: (1) Patients requiring aortic replacement. (2) Provided written informed consent and voluntarily agreed to take part in the study. (3) Males or nonpregnant females over 18 years of age. The exclusion criteria were: (1) Patients with an autoimmune disease. (2) Pregnant or lactating women. (3) Any other status or condition that would make participation in the study inappropriate.

2.2 Animals and Treatments

All animal experiments were approved by the Animal Care and Welfare Committee (Number: 20200326014) and were performed in adherence to the National Institutes of Health Guidelines for the Care and Use of Laboratory Animals and the ARRIVE guidelines. All animal procedures were conducted in strict compliance with the US National Institutes of Health Guide for the Care and Use of Laboratory Animals (8th Edition, 2011). Efforts were made to reduce the number of animals used and to minimize animal pain and discomfort. Macrophage-specific *Adam8* KO mice (Cyagen Biosciences, Suzhou, China) on a C57BL/6 background were generated using the Clustered Regularly Interspaced Short Palindromic Repeats/CRISPR-associated protein 9 (CRISPR/Cas9) system [24] (**Supplementary Fig. 1**). Mice were housed under controlled conditions at the Southeast University Laboratory Animal Center. They were maintained in a specific-pathogen-free environment within ventilated cages under a 12-hour light/dark cycle, with ad libitum access to food and water. Male mice aged 6–10 weeks were utilized in the current study. The study employed randomization with allocation concealment, and the operators were blinded to group assignment. Mice (n = 28) were fed a 0.25% adenine diet (Macklin, Shanghai, China) for 4 weeks to establish the CKD model. Subsequently, the CKD model mice were switched to a high-phosphorus diet (1.8% phosphorus; Xie Tong Sheng Wu) and received intramuscular injections of calcitriol (1 µg/kg; Sigma-Aldrich, Darmstadt, Germany) twice weekly to induce VC. A control group (n = 12) was maintained on a standard normal diet (ND) group (Xie Tong Sheng Wu, Nanjing, China) and received saline injections in parallel. Tail-tip blood sampling was performed at the start of the experiment (0 W), the fourth week (4 W), and the tenth week (10 W) without anesthesia. Prior to blood collection, the tails were immersed in warm water at approximately 50 °C and disinfected. After blood collection, hemostasis was applied, and the mice were adequately comforted. After 16 weeks, the mice were euthanized via an intraperitoneal injection of sodium pentobarbital (concentration 15 mg/mL, 200 mg/kg), and the aorta and blood were collected. At the conclusion of the experiment, surviving animals were transferred to other approved protocols within the institution for continued use.

2.3 Enzyme-Linked Immunosorbent Assay

Human plasma was processed by centrifugation (1000 rpm, 20 minutes, 4 °C) to pellet cellular debris, and the resulting supernatant was collected for subsequent analysis. Enzyme-linked immunosorbent assays (ELISAs) were performed according to the manufacturer's instructions (Elabscience Biotechnology Co., Ltd., Wuhan, China). Optical density (OD) was measured at a wavelength of 450 nm.

2.4 Histological Analysis

Following standard protocols, mouse aortas were paraffin-embedded and sectioned. For Von Kossa staining, sections were deparaffinized and rehydrated, then immersed in silver nitrate solution under ultraviolet light for 2 hours. After rinsing in phosphate-buffered saline (PBS), the sections were subjected to hematoxylin and eosin staining. Finally, all sections were dehydrated, mounted, and scanned using a digital slide scanner (Olympus VS200, Tokyo, Japan).

2.5 Immunofluorescence Imaging

Paraffin sections of human aortic tissue were prepared, dewaxed, and subjected to antigen retrieval. The tissue areas were outlined with a PAP Pen to prevent antibody dispersion. Sections were then incubated with the corresponding primary antibody at 4 °C overnight in a humidified chamber. After washing with PBS on a shaker, a secondary antibody was applied and incubated for 1 hour at room temperature. Nuclei were counterstained with 4′,6-diamidino-2-phenylindole. Following the application of an anti-fade mounting medium, the slides were coverslipped and imaged with a digital slide scanner (Olympus VS200). For quantitative analysis, five distinct regions of interest per sample were randomly selected at a higher magnification. The mean fluorescence intensity of ADAM8 and α-SMA within these regions was measured using ImageJ software (version 2; National Institutes of Health, Bethesda, MD, USA). Briefly, the mean fluorescence intensity was recorded for each of the five selected fields. The average fluorescence intensity per sample was then calculated from these five measurements. These sample averages were subsequently used to compare the differences between the non-calcified group (NG) and the calcified group (CG). Statistical analysis was performed using an unpaired two-tailed Student's *t*-test with GraphPad Prism 9.5.0 software (GraphPad Software, Inc. San Diego, CA, USA) and significance was set at $p < 0.05$.

2.6 Serum Measurements

The serum levels of creatinine, phosphorus, urea, calcium, ALP, as well as aortic calcium content, were mea-

sured using commercially available assay kits (Elabscience, Wuhan, China). Following the manufacturer's protocol, aortic tissue segments were lysed in the designated buffer. Calcium ions in the lysate were then chelated with methyl thymol blue under alkaline conditions to form a blue complex. The absorbance of the colored product was measured to quantify calcium content. The results were normalized to the total protein concentration determined with a BCA protein assay kit.

2.7 Construction of AAV Vector for Macrophage-Specific Adam8 overexpression (OE)

The AAV vector for macrophage-specific *Adam8* OE was generated by subcloning the mouse *Adam8* coding sequence (NM_007403) downstream of an EGFP-FT2A cassette into a GV650 backbone, under the control of a macrophage-specific F4/80 promoter (sequence provided in **Supplementary Information**). Briefly, the 3Flag sequence of GV650 was removed to generate a pAAV-F4/80p-EGFP-FT2A-NM_007403-SV40 PolyA construct. The *Adam8* fragment was amplified and inserted into the vector via NheI/EcoRI cloning sites. Following plasmid construction, recombinant AAV was packaged, purified, and its titer was determined, and cryopreserved at –80 °C (Genechem Co., Ltd., Shanghai, China). For *in vivo* delivery, 4 to 6-week-old male mice were administered approximately 8×10^{11} AAV viral genomes via a tail vein injection. After 4 weeks of AAV expression, the CKD-related VC model was induced in the mice. Animals were euthanized 16 weeks post-AAV injection for downstream analyses.

2.8 Western Blots

The aortic tissues were homogenized in RIPA lysis buffer supplemented with protease and phosphatase inhibitors (KeyGen Bio TECH, Nanjing, China). Equal amounts of total protein were loaded onto a pre-cast gel and separated by electrophoresis at a constant voltage of 120 V. Once the bromophenol blue dye front reached the bottom of the gel, proteins were transferred to polyvinylidene membranes using a rapid transfer system at 400 mA for 30 minutes. Following transfer, the membranes were blocked with 5% non-fat milk for 1 hour at room temperature. After blocking, membranes were trimmed and incubated overnight at 4 °C with the indicated primary antibodies. The next day, the membranes were washed and incubated with the corresponding horseradish peroxidase-conjugated secondary antibodies for 1 hour at room temperature with gentle shaking. Protein bands were visualized using an automated chemiluminescence imaging system (Tanon 5200, Shanghai, China). Band intensities were quantified with ImageJ software (version 2; National Institutes of Health, Bethesda, MD, USA), and statistical analysis was performed accordingly. Details of the antibodies used are provided in **Supplementary Table 2**.

2.9 Statistical Analysis

The sample sizes for both the clinical cohort and the mouse experiments were determined based on previously published studies with similar designs. Strict exclusion criteria were applied to the clinical cohort to minimize confounding factors and enhance the robustness of the results. Data analyses were performed using SPSS 26.0 (IBM, Armonk, NY, USA) and GraphPad Prism 9.5.0 software (GraphPad Software, Inc. San Diego, CA, USA).

Continuous data are presented as mean ± standard deviation. If data met the assumptions of both normality and homogeneity of variance, comparisons between two groups were analyzed using an unpaired *t*-test, while comparisons among more than two groups were assessed using one-way analysis of variance (ANOVA) followed by Tukey's or Student–Newman–Keuls post-hoc tests. For data that were normally distributed but had unequal variances, an unpaired *t*-test with Welch's correction was used for two-group comparisons, and Welch's ANOVA was applied for multiple-group comparisons. If data were not normally distributed, the Mann–Whitney test was used for two-group comparisons, and the Kruskal–Wallis test was used for multiple-group comparisons. Categorical variables were analyzed using the chi-squared test. Survival analysis was conducted using the Kaplan–Meier method, and differences between survival curves were evaluated using the log-rank test. A p-value of <0.05 was considered statistically significant.

3. Results

3.1 Plasma ADAM8 Levels Correlate With Renal Function and Aortic Calcification

Aortic calcification was used as the target lesion to explore the relationship between ADAM8 and VC. Ultimately, a total of 129 patients were enrolled for this segment of the research, including 85 CKD patients and 44 controls. Plasma samples were collected, and thoracoabdominal computed tomography (CT) scans were performed on all participants. The demographic and clinical characteristics of patients in both groups are presented in **Supplementary Table 1**. Patients in the CKD group exhibited higher neutrophil counts (5.21 ± 2.61 vs. 4.19 ± 1.29 × 10^9/L, $p = 0.003$), monocyte counts (0.49 ± 0.24 vs. 0.36 ± 0.13 × 10^9/L, $p < 0.001$), pan-immune-inflammation values (PIVs) (534.39 ± 622.395 vs. 286.45 ± 312.03, $p = 0.003$), systemic immune inflammation index (SII) values (1023.80 ± 1059.34 vs. 719.79 ± 569.77, $p = 0.036$), and plasma ADAM8 levels (942.74 ± 394.94 vs. 790.26 ± 237.05 pg/mL, $p = 0.007$) compared with the control group, along with lower lymphocyte counts (1.15 ± 0.52 vs. 1.46 ± 0.52 × 10^9/L, $p = 0.002$) and high-density lipoprotein cholesterol (HDL-C) levels (0.95 ± 0.39 vs. 1.18 ± 0.33 mmol/L, $p = 0.001$). Besides these differences and a reduced red blood cell count, as well as expected variations in renal function parameters, no other laboratory parameters differed significantly between the groups.

Table 1. Baseline characteristics of patients undergoing CT scans.

Characteristics	Non-VC group (n = 32)	VC group (n = 97)	*p*-value
Age (years)	53.91 ± 16.30	67.26 ± 9.55	<0.001***
Sex (male, n %)	20 (63%)	59 (61%)	0.867
Laboratory tests			
WBCs, $\times 10^9$/L	6.56 ± 1.52	6.98 ± 2.58	0.370
RBCs, $\times 10^{12}$/L	4.11 ± 0.83	3.89 ± 0.78	0.173
PLTs, $\times 10^9$/L	217.91 ± 74.81	186.77 ± 88.82	0.077
Neutrophils, $\times 10^9$/L	4.44 ± 1.37	5.00 ± 2.52	0.232
Lymphocytes, $\times 10^9$/L	1.51 ± 0.56	1.17 ± 0.51	0.002**
Monocytes, $\times 10^9$/L	0.41 ± 0.19	0.46 ± 0.23	0.240
ALT, U/L	20.13 ± 17.13	19.25 ± 19.16	0.819
AST, U/L	19.25 ± 8.06	22.83 ± 14.24	0.179
BUN, mmol/L	8.81 ± 7.44	12.67 ± 8.73	0.026*
Cr, mmol/L	225.97 ± 313.07	247.45 ± 239.61	0.685
UA, µmol/L	356.53 ± 177.99	362.84 ± 130.47	0.830
eGFR, mL/min/1.73 m^2	69.83 ± 41.21	48.18 ± 39.01	0.008**
TC, mmol/L	4.18 ± 1.29	3.49 ± 1.22	0.007**
TG, mmol/L	1.94 ± 1.97	1.51 ± 0.81	0.240
HDL-C, mmol/L	1.10 ± 0.35	1.01 ± 0.40	0.226
LDL-C, mmol/L	2.23 ± 0.83	1.86 ± 0.87	0.037*
HbA1c (%)	5.93 ± 1.61	6.50 ± 1.45	0.065
ADAM8, pg/mL	746.87 ± 310.93	1030.98 ± 488.49	0.008**
Indexes			
PIV	315.14 ± 278.46	494.25 ± 607.17	0.025*
SII	719.66 ± 444.25	986.23 ± 1036.20	0.045*

Values are presented as mean ± standard deviation, or n, and independent samples. The *t*-test was used for two-group comparisons. For categorical variables, the chi-squared test was used for comparisons. *$p < 0.05$, **$p < 0.01$, ***$p < 0.001$. Abbreviations: WBC, white blood cell; RBC, red blood cell; HbA1c, Hemoglobin A1c; PLT, platelet; BUN, blood urea nitrogen; UA, uric acid; Cr, serum creatinine; TC, total cholesterol; TG, triglycerides; LDL-C, low-density lipoprotein cholesterol; HDL-C, high-density lipoprotein cholesterol; PIV, pan-immune-inflammation value = (neutrophil count × platelet count × monocyte count) ÷ lymphocyte count; SII, systemic immune inflammation index = (platelet count × neutrophil count) ÷ lymphocyte count.

The chest and abdominal CT findings were used to categorize the participants into a calcified group (n = 97) and a non-calcified group (n = 32). Patients with aortic calcification were older (67.26 ± 9.55 vs. 53.91 ± 16.30 years, $p < 0.001$), had higher ADAM8 levels (1030.98 ± 488.49 vs. 746.87 ± 310.93 pg/mL, $p = 0.008$), blood urea nitrogen (BUN) levels (12.67 ± 8.73 vs. 8.81 ± 7.44 mmol/L, $p = 0.026$), PIV values (494.25 ± 607.17 vs. 315.14 ± 278.46, $p = 0.025$), and SII values (986.23 ± 1036.20 vs. 719.66 ± 444.25, $p = 0.045$) compared to the non-calcified group. Additionally, they had lower lymphocyte numbers (1.17 ± 0.51 vs. 1.51 ± 0.56 × 10^9/L, $p = 0.002$), estimated glomerular filtration rates (eGFRs) (48.18 ± 39.01 vs. 69.83 ± 41.21 mL/min/1.73 m^2, $p = 0.008$), total cholesterol (TC) (3.49 ± 1.22 vs. 4.18 ± 1.29 mmol/L, $p = 0.007$), and low-density lipoprotein cholesterol (LDL-C) levels (1.86 ± 0.87 vs. 2.23 ± 0.83 mmol/L, $p = 0.037$). The remaining parameters were not significantly different between the groups (Table 1).

3.2 ADAM8 Expression Is Significantly Increased in Calcified Arterial Tissue and Infiltrated Macrophages

We collected eight aortic tissue samples from patients who underwent aortic replacement to further analyze the relationship between ADAM8 and VC. The Von Kossa staining results were used to classify the samples into the aortic calcification group (AC) and the non-aortic calcification group (non-AC). The baseline demographic and clinical characteristics of the two groups are presented in Table 2. Patients in the AC group exhibited significantly higher uric acid (UA) levels (270.25 ± 32.69 vs. 185.75 ± 56.08 µmol/L, $p = 0.040$) and significantly lower eGFRs (66.51 ± 20.34 vs. 103.72 ± 4.14 mL/min/1.73 m^2, $p = 0.012$) compared to the non-AC group, while other indicators were comparable between groups. The results indicated that the AC group had poorer renal function.

Three adjacent sections from the same sample were respectively subjected to Von Kossa staining, immunofluorescence staining for ADAM8 and CD68 and immunofluo-

Table 2. Baseline characteristics of patients included for immunofluorescence staining.

Characteristics	AC (n = 4)	Non AC (n = 4)	*p*-value
Age (years)	67 ± 11.97	60.75 ± 1.5	0.374
Sex (male, n %)	3 (75%)	3 (75%)	1.000
WBCs, $\times 10^9$/L	8.56 ± 3.60	8.98 ± 3.68	0.876
RBCs, $\times 10^{12}$/L	3.46 ± 0.75	3.71 ± 1.01	0.690
PLTs, $\times 10^9$/L	202.50 ± 98.76	144.75 ± 102.34	0.448
Neutrophils, $\times 10^9$/L	6.88 ± 3.50	7.41 ± 3.73	0.843
Lymphocytes, $\times 10^9$/L	1.08 ± 0.31	1.37 ± 0.83	0.530
Monocytes, $\times 10^9$/L	0.55 ± 0.17	0.83 ± 0.33	0.212
ALT, U/L	64.25 ± 32.99	34.00 ± 30.21	0.225
AST, U/L	49.75 ± 43.60	33.00 ± 5.16	0.500
BUN, mmol/L	7.73 ± 1.39	6.33 ± 1.38	0.204
Cr, mmol/L	94.50 ± 19.91	64.75 ± 15.37	0.056
UA, µmol/L	270.25 ± 32.69	185.75 ± 56.08	0.040*
eGFR, mL/min/1.73 m^2	66.51 ± 20.34	103.72 ± 4.14	0.012*
TC, mmol/L	2.95 ± 0.96	3.43 ± 0.79	0.470
TG, mmol/L	1.46 ± 1.05	1.49 ± 0.65	0.960
HDL-C, mmol/L	0.90 ± 0.18	0.97 ± 0.26	0.655
LDL-C, mmol/L	1.61 ± 0.26	1.94 ± 0.80	0.456
FBG, mmol/L	7.36 ± 1.93	5.79 ± 0.68	0.204

Values are presented as mean ± standard deviation, or n%, and an independent samples *t*-test was used for two-group comparisons. For categorical variables, the chi-squared test was used for comparisons. *$p < 0.05$. Abbreviations: WBC, white blood cell; RBC, red blood cell; PLT, platelet; FBG, fasting blood glucose; BUN, blood urea nitrogen; UA, uric acid; Cr, serum creatinine; TC, total cholesterol; TG, triglycerides; LDL-C, low-density lipoprotein cholesterol; HDL-C, high-density lipoprotein cholesterol.

rescence staining for ADAM8 and α-SMA. The Von Kossa staining results were used to categorize the samples into a calcified group (CG) and a non-calcified group (NG). Subsequently, the vascular medial layer was regionally classified based on the results of CD68/ADAM8 immunofluorescence staining and the tissue structure. The CG was further divided into the calcified region, non-calcified region, and macrophage infiltration region, while the NG was partitioned into the non-calcified region and macrophage region.

Through comparative analysis, we observed that the calcified regions were co-localized with ADAM8, demonstrating significant ADAM8 expression (Fig. 1), and the expression level of ADAM8 was positively correlated with the degree of calcification (**Supplementary Fig. 2**). In the non-calcified regions of the CG, scattered ADAM8 expression was also detected, whereas no ADAM8 expression was observed in the tunica media in the NG (Fig. 1). In the CG, macrophage infiltration was evident around the calcified regions, termed the macrophage infiltration region, predominantly located within the medial layer. This region showed high ADAM8 expression in macrophages. In contrast, the macrophage region in the NG exhibited low ADAM8 expression, with a small number of macrophages, and this region was primarily localized at the junction between the intima and media (Fig. 2).

Immunofluorescence staining for both α-SMA and ADAM8 was performed to elucidate the source of ADAM8 in calcified medial tissues. The CG demonstrated a gradual decline in α-SMA expression within vascular tissues concomitant with VC development compared with the NG (Fig. 3 and **Supplementary Fig. 3**). Except for a small amount of ADAM8 and α-SMA co-localization around the macrophage infiltration region, a significant amount of ADAM8 was diffusely distributed among cells in the calcified regions, with no co-localization with α-SMA. In the NG, abundant α-SMA expression was detected in the medial layer, but no ADAM8 expression was observed (**Supplementary Fig. 4**). The NG predominantly exhibited atherosclerotic plaques, within which substantial ADAM8 expression was detected (**Supplementary Fig. 4**).

3.3 Macrophage Adam8 KO Inhibits Aortic Calcification in CKD Mice

We established macrophage-specific *Adam8* KO mice. Knocking out *Adam8* did not cause phenotypic changes in the mice. As shown in Fig. 4A, we established an *in vivo* CKD model using *Adam8* KO mice and control mice from the same litter. Knocking out macrophage *Adam8* KO did not affect the survival of mice in either sub-model group (Fig. 4B). As renal function deteriorated, the weight of the

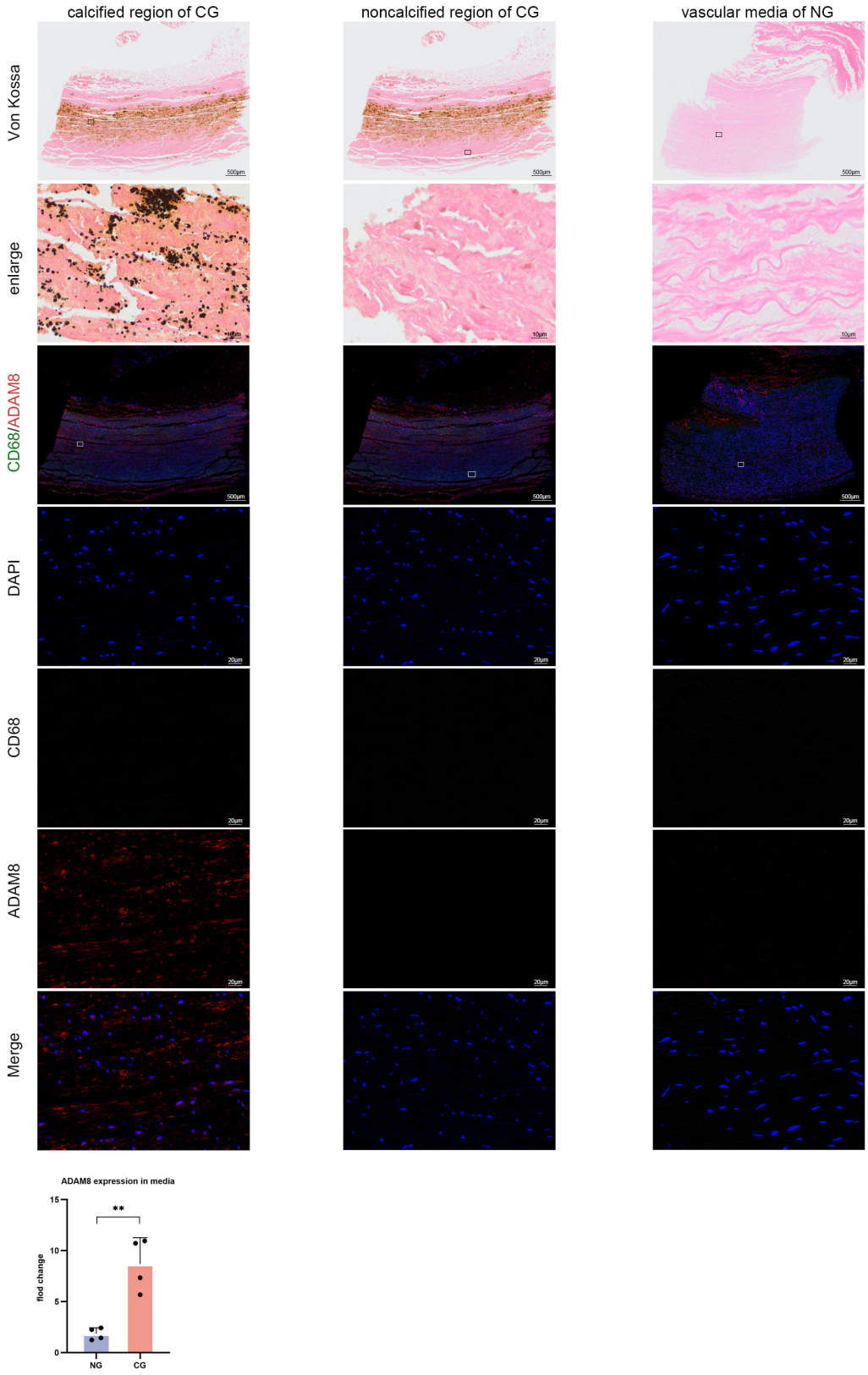

Fig. 1. Von Kossa staining images and immunofluorescence staining images of CD68 and ADAM8 in human aortic tissues. ADAM8 expression was co-localized with the calcified region, while hardly any ADAM8 expression was observed in non-calcified regions (n = 4) ($p = 0.0038$, unpaired t-test). $^{**}p < 0.01$. Abbreviation: ADAM8, A disintegrin and metalloproteinase 8; CD68, Cluster of differentiation 68; DAPI, 4′,6-Diamidino-2-Phenylindole. Scale bars: 500 µm (overview); 10 µm (Von Kossa); 20 µm (immunofluorescence staining).

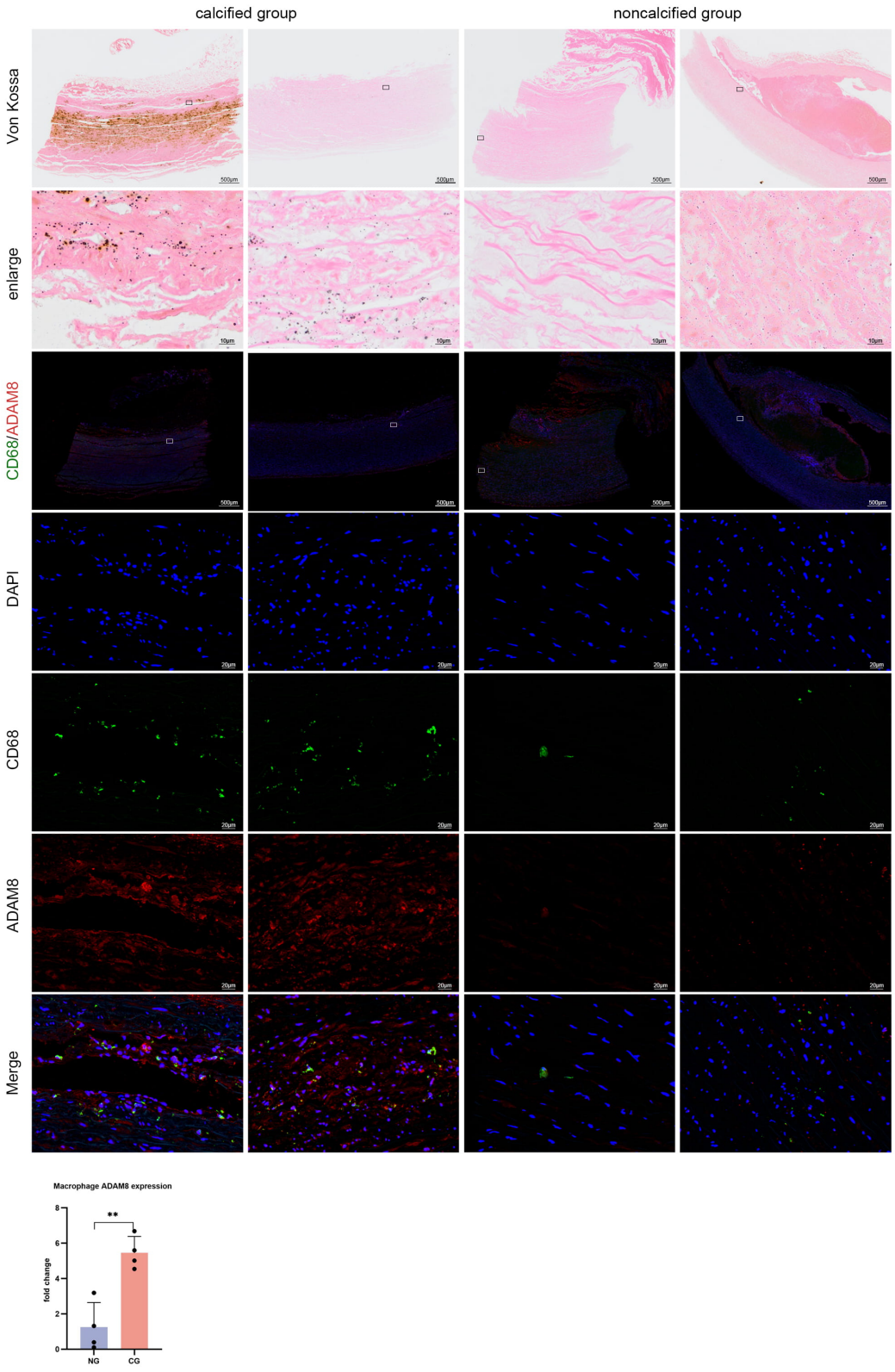

Fig. 2. Von Kossa staining images and CD68 and ADAM8 immunofluorescence staining images in human aortic samples. Comparison of Von Kossa staining and CD68 and ADAM8 immunofluorescence images between macrophage infiltration regions in the calcified group and macrophage regions in the non-calcified group revealed abundant ADAM8 expression in macrophage infiltration regions in the calcified group, while no such phenomenon was observed in the non-calcified group (n = 4) ($p = 0.0024$, unpaired t-test). $^{**}p < 0.01$. Abbreviations: ADAM8, A disintegrin and metalloproteinase 8; CD68, Cluster of differentiation 68; DAPI, 4′,6-Diamidino-2-Phenylindole. Scale bars: 500 μm (overview); 10 μm (Von Kossa); 20 μm (immunofluorescence staining).

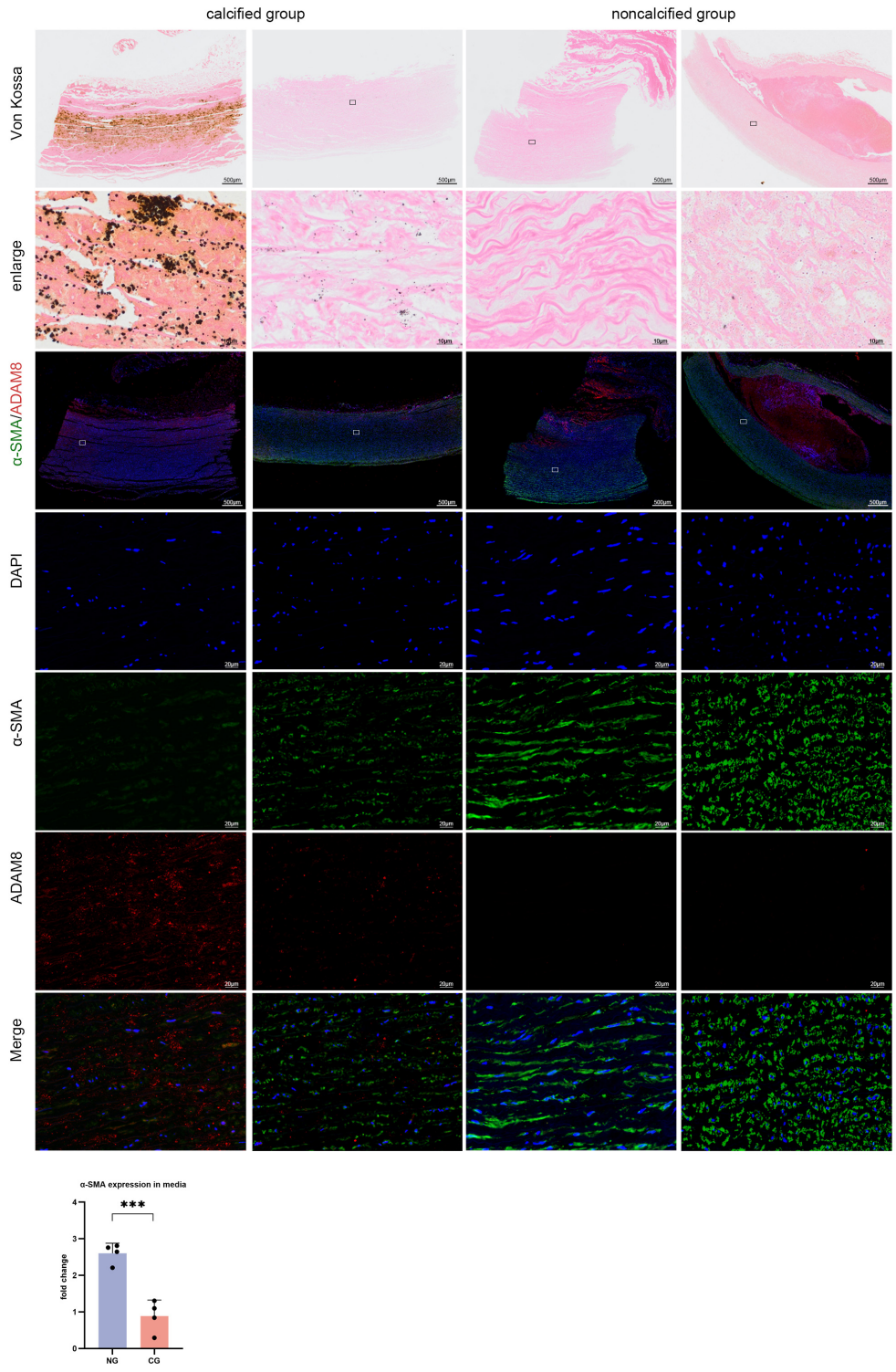

Fig. 3. Von Kossa staining images and immunofluorescence staining images of α-SMA and ADAM8 in human aortic tissues. Comparison of Von Kossa staining and α-SMA and ADAM8 immunofluorescence images between macrophage infiltration regions in the calcified group and macrophage regions in the non-calcified group revealed that as the degree of calcification increased, α-SMA expression decreased and ADAM8 expression increased (n = 4) ($p = 0.0006$, unpaired t-test). ***$p < 0.001$. Abbreviations: ADAM8, A disintegrin and metalloproteinase 8; α-SMA, alpha-smooth muscle actin; DAPI, 4′,6-Diamidino-2-Phenylindole. Scale bars: 500 µm (overview); 10 µm (Von Kossa); 20 µm (immunofluorescence staining).

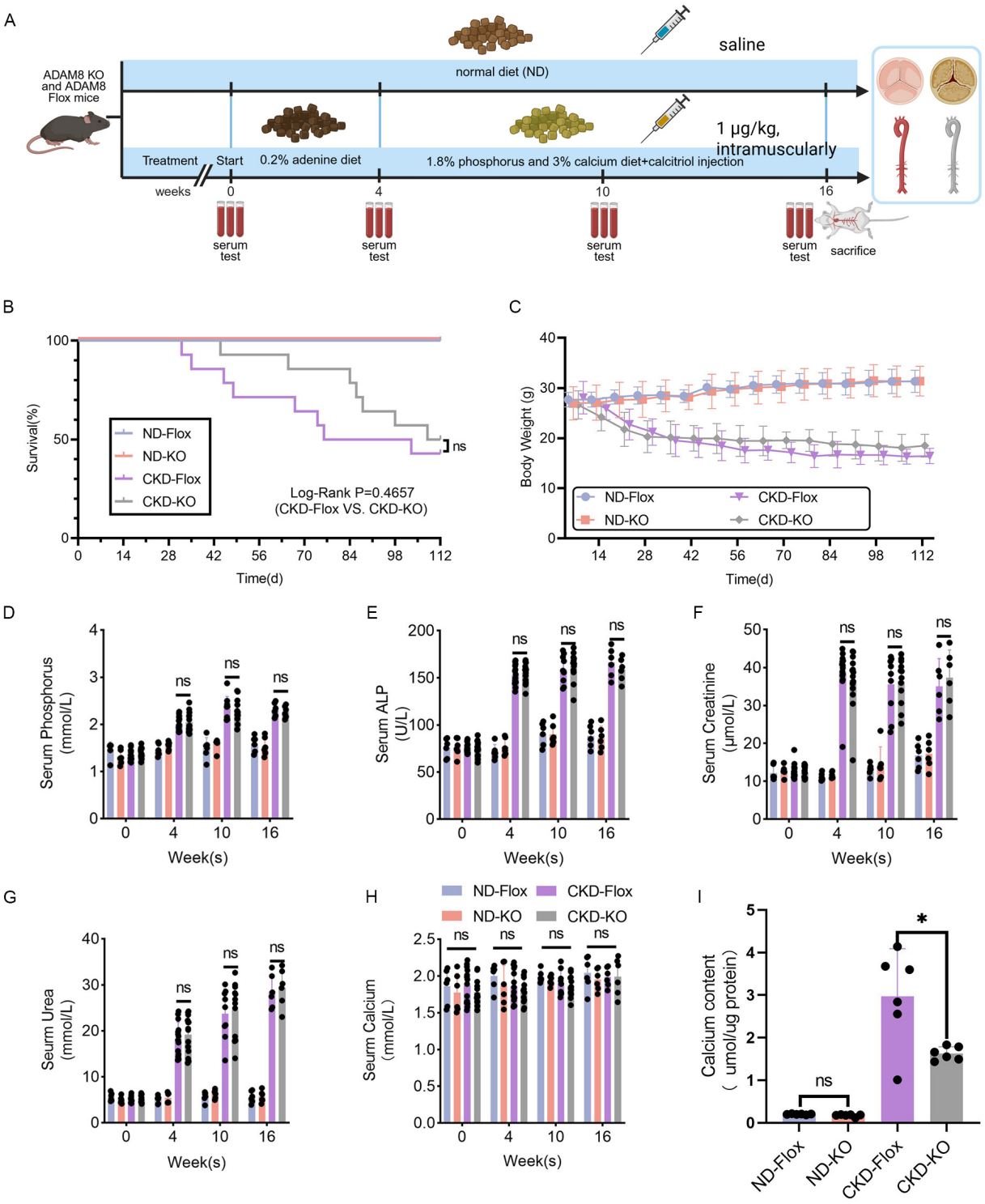

Fig. 4. *Adam8* KO has no protective effect on renal function in CKD mice. (A) Development of a mouse model for CKD-associated vascular calcification. Created in BioRender. Dong, R. (2025). https://BioRender.com/u16l265. (B) Survival curves. Cumulative mortality in the four groups of mice. ND-Flox mice (n = 6), ND-KO mice (n = 6), CKD-Flox mice (n = 14), and CKD-KO mice (n = 14). (C) Body weights (n = 6–14). (D) Biochemical analyses of serum phosphorus, serum alkaline phosphatase (ALP) (E), creatinine (F), urea (G), and calcium concentrations (H) at 0, 4, and 10 weeks during modeling. (I) Quantification of aortic tissue calcium content (n = 6–14). ($p = 0.015$, unpaired t-test). Notes: "n value" refers to the number of biological replicates. *$p < 0.05$. Abbreviations: KO, knockout; ND, normal diet. ns, no significant difference.

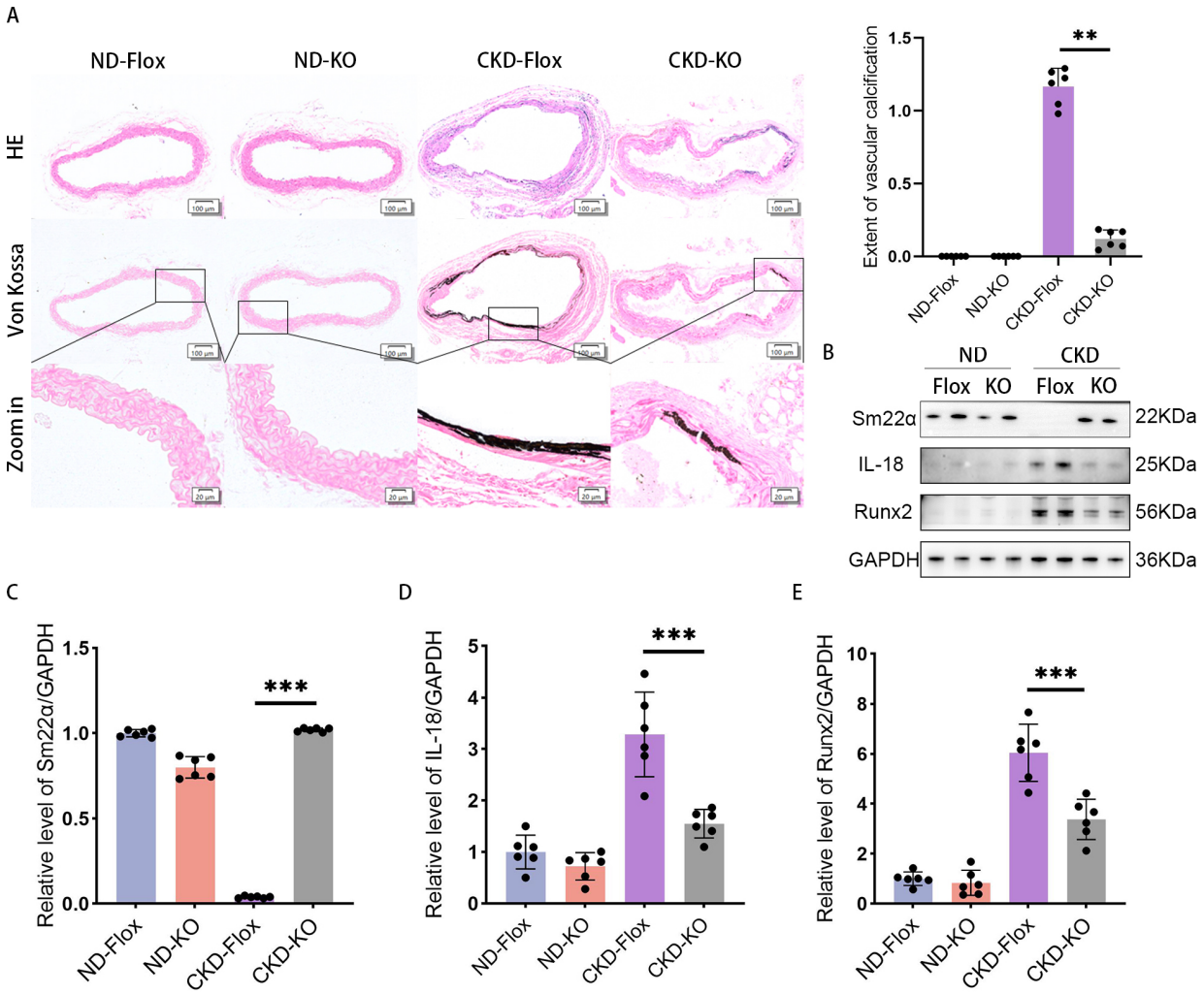

Fig. 5. Aortic calcification is attenuated by *Adam8* KO in CKD mice. (A) Representative Von Kossa staining images of vascular tissue from the four groups (positive staining: black) (n = 6). (B) Western blots of (C) SM22α ($p < 0.0001$ unpaired *t*-test; original blots/gels are presented in **Supplementary Figs. 6**,**7**), (D) Interleukin (IL)-18 ($p = 0.0006$ unpaired *t*-test), and (E) Runx2 in aortic tissues of the four groups of mice ($p = 0.0009$ unpaired *t*-test). Notes: "n value" refers to the number of biological replicates. $^{**}p < 0.01$, and $^{***}p < 0.001$. Abbreviations: HE, Hematoxylin and Eosin Staining; GAPDH, Glyceraldehyde-3-Phosphate Dehydrogenase; SM22α, smooth muscle protein 22-alpha; Runx2, Runt-related transcription factor 2. Scale bars: 100 µm (overview); 20 µm (high magnification).

mice in both model groups decreased equally (Fig. 4C). At the beginning of the experiment (0 weeks), as well as at the fourth and tenth weeks, we evaluated renal function impairment. The results showed that serum phosphorus (Fig. 4D), ALP (Fig. 4E), creatinine (Fig. 4F), and urea (Fig. 4G) levels were significantly elevated in both model groups, with no statistically significant differences observed between the two groups. No significant differences in serum calcium levels were observed among the four groups (Fig. 4H), suggesting that the adenine diet was successful in inducing renal injury and that the KO of macrophage-specific *Adam8* did not alter renal function. The aortic calcium content in both CKD groups was increased compared with the ND groups and was higher in the CKD-Flox group than in the CKD-KO group (Fig. 4I).

The extent of VC in the aortic media was assessed by Von Kossa staining and measuring the calcium content. We dissected mice that died during the experiment and compared the calcification of the aortic valve and aorta in the two sub-model groups. Calcification occurred earlier in the aortic valves than in the aortic vessels. Furthermore, the valvular calcification was more severe in the CKD-Flox group compared to the CKD-KO group (**Supplementary Fig. 5**). The CKD-Flox group displayed more severe vascular calcification than the CKD-KO group (Fig. 5A). Western blots (Fig. 5B and **Supplementary Figs. 6**,**7**) showed that Runx2 expression was increased in vascular tissue in the CKD groups (Fig. 5E) Sm22α expression was decreased (Fig. 5C) compared with the ND groups. The CKD-Flox group had higher Runx2 expression and lower Sm22α expression than with CKD-KO group. Given that CKD is an

inflammatory disease and that ADAM8 is also related to inflammation, we examined the expression of inflammation-related markers. Interleukin (IL)-18 expression was significantly elevated in the CKD-Flox group (Fig. 5D). This suggests that *Adam8* KO may attenuate vascular calcification by suppressing inflammation.

3.4 Macrophage-Specific OE of ADAM8 Prevents Improvements in Vascular Calcification Achieved by Adam8 KO

The association between macrophage-derived ADAM8 and VC was investigated using macrophage-specific *Adam8* OE. This was achieved by injecting the tail veins of 4-week-old *Adam8* KO mice with either AAV6-F4/80-*Adam8* or a control virus. Following viral delivery, CKD-associated VC was induced in these animals. The results showed that the mice successfully overexpressed ADAM8 after viral injection (Fig. 6B,C and **Supplementary Fig. 8**). VC was significantly aggravated in the CKD+KO+OE group compared to the CKD+KO+NC group (Fig. 6A). Consistent with this phenotypic enhancement, Western blot analysis revealed a concurrent upregulation of osteogenic (Runx2) and inflammatory (IL-18) markers, and a downregulation of Sm22α in the aortic tissues of the CKD+KO+OE mice (Fig. 6D–G, **Supplementary Figs. 9,10**).

4. Discussion

Vascular calcification is very common in elderly people and CKD populations, and has become a potential killer in seniors due to a lack of sufficient attention and effective prevention and treatment [25,26]. VC has also been associated with cognitive decline [27,28]. The dual threat of VC to long-term health and quality of life has increased its social burden in the context of an aging society and population. Deciphering the mechanisms of VC can lay a foundation for its prevention and targeted treatment. Here, our study demonstrated a relationship between macrophage ADAM8 and VC, and macrophage-specific *Adam8* KO attenuated VC in CKD model mice. These findings extend beyond identifying a regulatory role for ADAM8 in VC to provide novel evidence for the macrophage-mediated regulation of this pathological process.

ADAM8 is a shedding enzyme that is involved in a series of physiological and pathological processes, such as ovulation, inflammation, tumor metastasis, and progression. ADAM8 is not essential for homeostasis, and it is expressed at very low levels in normal conditions. It can be found in either a transmembrane location or in a soluble form. Previous studies have shown that serum ADAM8 levels are dramatically increased in various inflammatory diseases such as asthma, COPD [22,29], gingivitis [30], periprosthetic inflammation of the hip joint [31], and neoplastic diseases [20]. In addition, serum or tissue fluid levels of ADAM8 have been shown to correlate with disease severity. Although inhibiting or knocking down *Adam8* was shown to decrease inflammatory responses or slow tumor metastasis [32,33], it is not clear whether ADAM8 deficiency inhibits VC. Considering that VC is an inflammatory disease and ADAM8 is associated with inflammation, we hypothesized that ADAM8 promotes VC.

First, we included CKD patients and controls. We found that elevated plasma ADAM8 levels were associated with poorer renal function. The participants were categorized into VC and non-VC groups according to the CT scan findings. A comparison of the two groups found that aortic calcification was associated with age and plasma ADAM8 levels. Previous studies have identified a correlation between plasma ADAM8 levels and aortic calcification. Notably, patients with vascular calcification accompanied by renal dysfunction exhibited significantly elevated plasma ADAM8 concentrations.

Our previous work found that plasma ADAM8 is associated with inflammation, renal function, and aortic calcification, and various risk factors, including aging, smoking, diabetes, and hypertension, can lead to VC. As a result of its inflammatory nature, the chronic progression of VC leads to a state of sustained, low-grade innate immune activation. This persistent signaling ultimately drives maladaptive tissue responses [34]. Closely linked and critically involved in VC [34], macrophages play essential roles in its onset, progression, and regression [19]. Furthermore, alterations in the tissue microenvironment can lead to adaptive responses in macrophages, with different polarities, phenotypes, or secretome profiles. Given that the infiltration of monocytes/macrophages into vascular tissues is a key step in the formation of VC, through a variety of mechanisms, we chose to perform Von Kossa staining and immunofluorescence staining of CD68, ADAM8, and α-Sma on aortic tissue samples from patients who underwent aortic replacement.

The staining results showed that the calcified vascular intima-media tissue area co-localized with ADAM8 and there was a high prevalence of ADAM8-positive macrophages infiltrating around the calcified vascular tissues (Fig. 1). On the one hand, this finding corroborated that VC is associated with macrophage infiltration, and on the other hand, we found that the infiltration of macrophages into the vascular intima-media might promote VC by releasing ADAM8. A large amount of ADAM8 expression was found in the vicinity of atherosclerotic lipid plaques, accompanied by high macrophage infiltration. Both inflammatory diseases exhibited the release of ADAM8, but the sites where macrophages infiltrated and released ADAM8 differed.

The immunofluorescence imaging of α-SMA and ADAM8 showed co-localization primarily around ADAM8-positive macrophages. Accumulating evidence indicates that macrophages drive vascular calcification by modulating the phenotype of adjacent VSMCs [35–37].

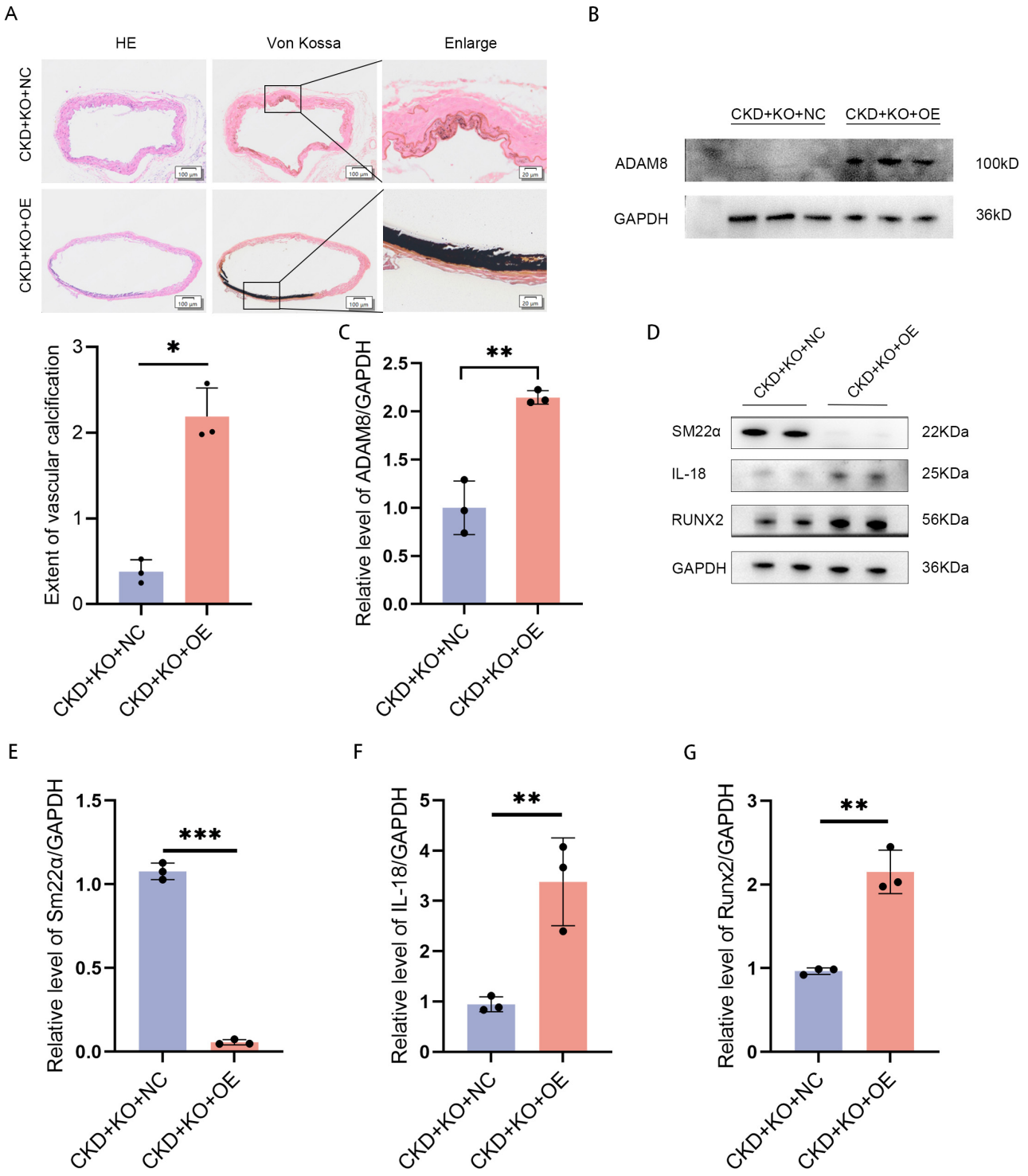

Fig. 6. *Adam8* OE exacerbates aortic calcification in *Adam8* KO mice under CKD conditions. (A) Representative images of Von Kossa staining in the aortic tissues of mice from the two CKD groups (positive staining: black). (B) Western blot analysis and (C) quantification of ADAM8 protein levels ($p < 0.01$, unpaired *t*-test; original blots/gels are presented in **Supplementary Fig. 10**). (D) Western blot analysis and quantification of (E) Sm22α protein levels ($p < 0.001$, unpaired *t*-test; original blots/gels are presented in **Supplementary Figs. 8**,**9**); (F) Interleukin (IL)-18 ($p = 0.0089$, unpaired *t*-test); and (G) Runx2 in mouse aortic tissues ($p = 0.0014$, unpaired *t*-test) (n = 3). *$p < 0.05$, **$p < 0.01$, and ***$p < 0.001$. Notes: "n value" refers to the number of biological replicates. Scale bars: 100 µm (overview); 20 µm (high magnification).

The infiltration of ADAM8-positive macrophages and their aggregation around calcified vascular tissues, in addition to the co-localization of ADAM8 with the site of VC, strongly suggest an association between macrophage ADAM8 and VC.

Whether ADAM8 is a participant or a bystander in cardiovascular disease is still under debate. Because ADAM8 is widely involved in inflammatory responses and exists in both transmembrane and soluble forms, studies of one form of ADAM8 do not reflect its complete function. Second, ADAM8 contains multiple structural domains, each of which can exercise different functions [38]. Nevertheless, the general consensus is that serum ADAM8 levels correlate with the severity of cardiovascular disease [21]. Theodorou *et al.* [39] found that ADAM8 was associated with plaque progression in humans, but systemic and hematopoietic ADAM8 deficiency did not affect the development of advanced atherosclerotic lesions. In addition, ADAM8 expression was most prominent in the shoulder region of human atherosclerotic lesions [39]. Elevated serum ADAM8 levels were associated with postoperative organ dysfunction in coronary artery disease patients [21].

In this study, we found a correlation between plasma ADAM8 levels and aortic calcification in patients with CKD. Furthermore, tissue samples showed that ADAM8 was enriched in human calcified arterial tissue, and there was high infiltration of ADAM8-positive macrophages around calcified vascular tissues, strongly suggesting that macrophage ADAM8 may contribute to VC development.

Although ADAM8 is essential in homeostasis, ADAM8 deficiency does not cause a phenotypic shift, and *Adam8* KO mice show only mild developmental defects, as well as increased neovascularization in a model of retinopathy under oxygen-induced conditions [40]. Therefore, we constructed macrophage-specific *Adam8* KO mice to further investigate the relationship between ADAM8 and VC. We chose the CKD model, an accelerated model of aging [41–43], to validate the relationship between ADAM8 and VC. The CKD groups of mice were first subjected to renal function impairment. The hematological index tests during modeling suggested that the renal function of mice in the model groups was impaired to similar extents. *Adam8* KO had no effect on renal function impairment, body weight change, or survival rates during modeling. Autopsies of the mice that died during modeling revealed that mice in the CKD-Flox group first developed aortic valve calcification. Von Kossa staining of the aorta in all four groups of mice suggested that VC was more severe in the CKD-Flox group than in the CKD-KO group, while tissue Western blotting suggested that calcification proteins (such as Runx2) were increased and contractile markers (such as Sm22α) were decreased. In contrast, the pathological vascular phenotype observed in the model groups was ameliorated in the CKD-KO group. Subsequent validation demonstrated significantly lower IL-18 levels in vascular tissues in the KO group, consistent with the observed phenotypic improvement. IL-18 is an important pro-vascular calcification factor [44,45], and *Adam8* KO led to a decrease in the levels of IL-18, which attenuated the occurrence of VC.

Finally, we performed rescue experiments by overexpressing macrophage ADAM8 by injecting AAV virus into the tail vein of *Adam8* KO mice. Four weeks later, CKD-related VC was induced in the mice. Mice in the CKD+KO+OE group exhibited significantly aggravated VC compared to the CKD+KO+NC group (Fig. 6A). Furthermore, the Western blotting data suggested that the expression of Runx2 and IL-18 was elevated in arterial tissues, and Sm22α was decreased, further suggesting that ADAM8 could lead to the development of VC via IL-18 under inflammatory conditions.

5. Limitations

The present study still has shortcomings. For example, aging and VC development have long-term chronic courses, and our model was different from the normal aging process. Additionally, there was a limitation in the design of our rescue experiment. We employed the F4/80 promoter to drive macrophage-specific ADAM8 expression. Although F4/80 is a valuable pan-macrophage marker, its broad activity in various tissue-resident macrophages, particularly the abundant Kupffer cells in the liver, introduces a potentially confounding factor. For instance, inducing ADAM8 expression in Kupffer cells may alter their functions, such as cytokine secretion, the clearance of circulating metabolites, and overall liver homeostasis. This hepatic alteration presents a plausible indirect mechanism that could influence our primary observation—the modulation of VC. An impaired or activated liver may systemically release a cascade of factors, including pro-inflammatory cytokines, uremic toxins in the context of renal impairment, or dysregulated calcification mediators such as Fetuin-A or Matrix Gla Protein, all of which are known to profoundly affect the VC process [46]. Therefore, although our data robustly demonstrated that ADAM8 re-expression rescued the VC phenotype in CKD, it failed to further distinguish the direct local effects of macrophage ADAM8 from the indirect effects mediated by systemic signals originating from the liver. Future studies utilizing more spatially restricted macrophage-specific promoters, such as those targeting plaque macrophages, or bone marrow transplantation models, combined with the direct analysis of liver function and systemic cytokine and adipokine profiles, will be essential to dissecting local versus systemic mechanisms and fully elucidating the role of ADAM8 in this complex pathology.

6. Conclusions

The present study revealed the relationship between macrophage ADAM8 and VC, as well as the potential

role of macrophage ADAM8 in the pathogenesis of VC. Macrophage ADAM8 deletion slowed the CKD-induced VC. ADAM8 deletion might attenuate VC by decreasing the expression of IL-18. Combined with these results, ADAM8 inhibition or KO may have some preventive potential in VC.

Availability of Data and Materials

The original data of the study are appended to the article/**Supplementary Material**. All data reported in this paper will also be shared by the lead contact upon request.

Author Contributions

RD, ZJJ and GSM designed the research study. RD, MW, ZXT and XXL performed the research. ZXT, XXL and JWX participated in the acquisition of date. RD and RZ analyzed the data. RD and ZJJ wrote the manuscript. All authors contributed to editorial changes in the manuscript. All authors read and approved the final manuscript. All authors have participated sufficiently in the work and agreed to be accountable for all aspects of the work.

Ethics Approval and Consent to Participate

The study was conducted in accordance with the Declaration of Helsinki. The research protocol was approved by the Ethics Committee of Southeast University affiliated Zhongda Hospital (Number: 2023ZDSYLL298-P01) (Number: 2024ZDSYLL150-P01). All of the participants provided signed informed consent. Besides, all animal experiments were performed in accordance with the US National Institutes of Health Guide for the Care and Use of Laboratory Animals (8th Edition, 2011). All animal experiments conformed to animal experimental ethics rules and were approved by the Animal Care & Welfare Committee of Southeast University (Number: 20200326014).

Acknowledgment

We are grateful to the staff in Biobank of Zhongda Hospital, School of Medicine, Southeast University for technical assistance. We thank Cyagen Biosciences Co., Ltd. (Suzhou, China) for technical assistance in generation of macrophage-specific Adam8-KO mice. Graphical protocols for modeling are Created with BioRender.com (Agreement number: YZ27OEY0B4). We thank the contribution of BioRender in help us creating Graphical Protocols. We greatly appreciate the patients who willingly participated in this study.

Funding

This report was funded by Jiangsu Provincial Key Research and Development Program (BE2022852) and Research Personnel Cultivation Program of Zhongda Hospital Southeast University (CZXM-GSP-RC167).

Conflict of Interest

The authors declare no conflict of interest.

Supplementary Material

Supplementary material associated with this article can be found, in the online version, at https://doi.org/10.31083/FBL49495.

References

[1] Xu C, Smith ER, Tiong MK, Ruderman I, Toussaint ND. Interventions To Attenuate Vascular Calcification Progression in Chronic Kidney Disease: A Systematic Review of Clinical Trials. Journal of the American Society of Nephrology. 2022; 33: 1011–1032. https://doi.org/10.1681/ASN.2021101327.

[2] Li X, Liu A, Xie C, Chen Y, Zeng K, Xie C, *et al*. The transcription factor GATA6 accelerates vascular smooth muscle cell senescence-related arterial calcification by counteracting the role of anti-aging factor SIRT6 and impeding DNA damage repair. Kidney International. 2024; 105: 115–131. https://doi.org/10.1016/j.kint.2023.09.028.

[3] Liu X, Chen A, Liang Q, Yang X, Dong Q, Fu M, *et al*. Spermidine inhibits vascular calcification in chronic kidney disease through modulation of SIRT1 signaling pathway. Aging Cell. 2021; 20: e13377. https://doi.org/10.1111/acel.13377.

[4] Zheng G, Zhao Y, Li Z, Hua Y, Zhang J, Miao Y, *et al*. GLSP and GLSP-derived triterpenes attenuate atherosclerosis and aortic calcification by stimulating ABCA1/G1-mediated macrophage cholesterol efflux and inactivating RUNX2-mediated VSMC osteogenesis. Theranostics. 2023; 13: 1325–1341. https://doi.org/10.7150/thno.80250.

[5] Byun KA, Oh S, Yang JY, Lee SY, Son KH, Byun K. Ecklonia cava extracts decrease hypertension-related vascular calcification by modulating PGC-1α and SOD2. Biomedicine & Pharmacotherapy. 2022; 153: 113283. https://doi.org/10.1016/j.biopha.2022.113283.

[6] Lanzer P, Hannan FM, Lanzer JD, Janzen J, Raggi P, Furniss D, *et al*. Medial Arterial Calcification: JACC State-of-the-Art Review. Journal of the American College of Cardiology. 2021; 78: 1145–1165. https://doi.org/10.1016/j.jacc.2021.06.049.

[7] Ma W, Jia K, Cheng H, Xu H, Li Z, Zhang H, *et al*. Orphan Nuclear Receptor NR4A3 Promotes Vascular Calcification via Histone Lactylation. Circulation Research. 2024; 134: 1427–1447. https://doi.org/10.1161/CIRCRESAHA.123.323699.

[8] Bourne LE, Wheeler-Jones CP, Orriss IR. Regulation of mineralisation in bone and vascular tissue: a comparative review. The Journal of Endocrinology. 2021; 248: R51–R65. https://doi.org/10.1530/JOE-20-0428.

[9] Cannata-Andia JB, Roman-Garcia P, Hruska K. The connections between vascular calcification and bone health. Nephrology Dialysis Transplantation. 2011; 26: 3429–3436. https://doi.org/10.1093/ndt/gfr591.

[10] Jiang W, Zhang Z, Li Y, Chen C, Yang H, Lin Q, *et al*. The Cell Origin and Role of Osteoclastogenesis and Osteoblastogenesis in Vascular Calcification. Frontiers in Cardiovascular Medicine. 2021; 8: 639740. https://doi.org/10.3389/fcvm.2021.639740.

[11] Zhai X, Cao S, Wang J, Qiao B, Liu X, Hua R, *et al*. Carbonylation of Runx2 at K176 by 4-Hydroxynonenal Accelerates Vascular Calcification. Circulation. 2024; 149: 1752–1769. https://doi.org/10.1161/CIRCULATIONAHA.123.065830.

[12] Liu Y, Shanahan CM. Signalling pathways and vascular calcification. Frontiers in Bioscience (Landmark Edition). 2011; 16: 1302–1314. https://doi.org/10.2741/3790.

[13] Li XF, Wang Y, Zheng DD, Xu HX, Wang T, Pan M, *et al*.

M1 macrophages promote aortic valve calcification mediated by microRNA-214/TWIST1 pathway in valvular interstitial cells. American Journal of Translational Research. 2016; 8: 5773–5783.

[14] Ma WQ, Sun XJ, Zhu Y, Liu NF. PDK4 promotes vascular calcification by interfering with autophagic activity and metabolic reprogramming. Cell Death & Disease. 2020; 11: 991. https://doi.org/10.1038/s41419-020-03162-w.

[15] Ma WQ, Sun XJ, Zhu Y, Liu NF. Metformin attenuates hyperlipidaemia-associated vascular calcification through anti-ferroptotic effects. Free Radical Biology & Medicine. 2021; 165: 229–242. https://doi.org/10.1016/j.freeradbiomed.2021.01.033.

[16] Ye Y, Chen A, Li L, Liang Q, Wang S, Dong Q, *et al*. Repression of the antiporter SLC7A11/glutathione/glutathione peroxidase 4 axis drives ferroptosis of vascular smooth muscle cells to facilitate vascular calcification. Kidney International. 2022; 102: 1259–1275. https://doi.org/10.1016/j.kint.2022.07.034.

[17] Wang PW, Pang Q, Zhou T, Song XY, Pan YJ, Jia LP, *et al*. Irisin alleviates vascular calcification by inhibiting VSMC osteoblastic transformation and mitochondria dysfunction via AMPK/Drp1 signaling pathway in chronic kidney disease. Atherosclerosis. 2022; 346: 36–45. https://doi.org/10.1016/j.atherosclerosis.2022.02.007.

[18] Rao Z, Zheng Y, Xu L, Wang Z, Zhou Y, Chen M, *et al*. Endoplasmic Reticulum Stress and Pathogenesis of Vascular Calcification. Frontiers in Cardiovascular Medicine. 2022; 9: 918056. https://doi.org/10.3389/fcvm.2022.918056.

[19] Li Y, Sun Z, Zhang L, Yan J, Shao C, Jing L, *et al*. Role of Macrophages in the Progression and Regression of Vascular Calcification. Frontiers in Pharmacology. 2020; 11: 661. https://doi.org/10.3389/fphar.2020.00661.

[20] Mierke CT. The versatile roles of ADAM8 in cancer cell migration, mechanics, and extracellular matrix remodeling. Frontiers in Cell and Developmental Biology. 2023; 11: 1130823. https://doi.org/10.3389/fcell.2023.1130823.

[21] Schick D, Babendreyer A, Wozniak J, Awan T, Noels H, Liehn E, *et al*. Elevated expression of the metalloproteinase ADAM8 associates with vascular diseases in mice and humans. Atherosclerosis. 2019; 286: 163–171. https://doi.org/10.1016/j.atherosclerosis.2019.03.008.

[22] Ainola M, Li TF, Mandelin J, Hukkanen M, Choi SJ, Salo J, *et al*. Involvement of a disintegrin and a metalloproteinase 8 (ADAM8) in osteoclastogenesis and pathological bone destruction. Annals of the Rheumatic Diseases. 2009; 68: 427–434. https://doi.org/10.1136/ard.2008.088260.

[23] Ishizuka H, García-Palacios V, Lu G, Subler MA, Zhang H, Boykin CS, *et al*. ADAM8 enhances osteoclast precursor fusion and osteoclast formation in vitro and in vivo. Journal of Bone and Mineral Research. 2011; 26: 169–181. https://doi.org/10.1002/jbmr.199.

[24] Ji Z, Guo J, Zhang R, Zuo W, Xu Y, Qu Y, *et al*. ADAM8 deficiency in macrophages promotes cardiac repair after myocardial infarction via ANXA2-mTOR-autophagy pathway. Journal of Advanced Research. 2025; 73: 483–499. https://doi.org/10.1016/j.jare.2024.07.037.

[25] Singh A, Tandon S, Tandon C. An update on vascular calcification and potential therapeutics. Molecular Biology Reports. 2021; 48: 887–896. https://doi.org/10.1007/s11033-020-06086-y.

[26] Wu M, Rementer C, Giachelli CM. Vascular calcification: an update on mechanisms and challenges in treatment. Calcified Tissue International. 2013; 93: 365–373. https://doi.org/10.1007/s00223-013-9712-z.

[27] Sun Z, Liu J, Sun J, Xu Z, Liu W, Mao N, *et al*. Decreased Regional Spontaneous Brain Activity and Cognitive Dysfunction in Patients with Coronary Heart Disease: a Resting-state Functional MRI Study. Academic Radiology. 2023; 30: 1081–1091. https://doi.org/10.1016/j.acra.2022.11.022.

[28] Gadde KM, Yin X, Goldberg RB, Orchard TJ, Schlögl M, Dabelea D, *et al*. Coronary Artery Calcium and Cognitive Decline in the Diabetes Prevention Program Outcomes Study. Journal of the American Heart Association. 2023; 12: e029671. https://doi.org/10.1161/JAHA.123.029671.

[29] Lee SY, Chao CT, Huang JW, Huang KC. Vascular Calcification as an Underrecognized Risk Factor for Frailty in 1783 Community-Dwelling Elderly Individuals. Journal of the American Heart Association. 2020; 9: e017308. https://doi.org/10.1161/JAHA.120.017308.

[30] Nimcharoen T, Aung WPP, Makeudom A, Sastraruji T, Khongkhunthian S, Sirinirund B, *et al*. Reduced ADAM8 levels upon non-surgical periodontal therapy in patients with chronic periodontitis. Archives of Oral Biology. 2019; 97: 137–143. https://doi.org/10.1016/j.archoralbio.2018.10.021.

[31] Mandelin J, Li TF, Hukkanen MVJ, Liljeström M, Chen ZK, Santavirta S, *et al*. Increased expression of a novel osteoclast-stimulating factor, ADAM8, in interface tissue around loosened hip prostheses. The Journal of Rheumatology. 2003; 30: 2033–2038.

[32] Conrad C, Yildiz D, Cleary SJ, Margraf A, Cook L, Schlomann U, *et al*. ADAM8 signaling drives neutrophil migration and ARDS severity. JCI Insight. 2022; 7: e149870. https://doi.org/10.1172/jci.insight.149870.

[33] Romagnoli M, Mineva ND, Polmear M, Conrad C, Srinivasan S, Loussouarn D, *et al*. ADAM8 expression in invasive breast cancer promotes tumor dissemination and metastasis. EMBO Molecular Medicine. 2014; 6: 278–294. https://doi.org/10.1002/emmm.201303373.

[34] Passos LSA, Lupieri A, Becker-Greene D, Aikawa E. Innate and adaptive immunity in cardiovascular calcification. Atherosclerosis. 2020; 306: 59–67. https://doi.org/10.1016/j.atherosclerosis.2020.02.016.

[35] Cochain C, Vafadarnejad E, Arampatzi P, Pelisek J, Winkels H, Ley K, *et al*. Single-Cell RNA-Seq Reveals the Transcriptional Landscape and Heterogeneity of Aortic Macrophages in Murine Atherosclerosis. Circulation Research. 2018; 122: 1661–1674. https://doi.org/10.1161/CIRCRESAHA.117.312509.

[36] Chen Y, Waqar AB, Nishijima K, Ning B, Kitajima S, Matsuhisa F, *et al*. Macrophage-derived MMP-9 enhances the progression of atherosclerotic lesions and vascular calcification in transgenic rabbits. Journal of Cellular and Molecular Medicine. 2020; 24: 4261–4274. https://doi.org/10.1111/jcmm.15087.

[37] Li Q, Zhang C, Shi J, Yang Y, Xing X, Wang Y, *et al*. High-Phosphate-Stimulated Macrophage-Derived Exosomes Promote Vascular Calcification via let-7b-5p/TGFBR1 Axis in Chronic Kidney Disease. Cells. 2022; 12: 161. https://doi.org/10.3390/cells12010161.

[38] van der Vorst EPC, Donners MMPC. ADAM8 in the cardiovascular system: An innocent bystander with clinical use? Atherosclerosis. 2019; 286: 147–149. https://doi.org/10.1016/j.atherosclerosis.2019.04.205.

[39] Theodorou K, van der Vorst EPC, Gijbels MJ, Wolfs IMJ, Jeurissen M, Theelen TL, *et al*. Whole body and hematopoietic ADAM8 deficiency does not influence advanced atherosclerotic lesion development, despite its association with human plaque progression. Scientific Reports. 2017; 7: 11670. https://doi.org/10.1038/s41598-017-10549-x.

[40] Zhang Y, Tian Z, Gerard D, Yao L, Shofer FS, Cs-Szabo G, *et al*. Elevated inflammatory gene expression in intervertebral disc tissues in mice with ADAM8 inactivated. Scientific Reports. 2021; 11: 1804. https://doi.org/10.1038/s41598-021-81495-y.

[41] Hobson S, Arefin S, Kublickiene K, Shiels PG, Stenvinkel P.

Senescent Cells in Early Vascular Ageing and Bone Disease of Chronic Kidney Disease-A Novel Target for Treatment. Toxins. 2019; 11: 82. https://doi.org/10.3390/toxins11020082.

[42] Fang YP, Zhao Y, Huang JY, Yang X, Liu Y, Zhang XL. The functional role of cellular senescence during vascular calcification in chronic kidney disease. Frontiers in Endocrinology. 2024; 15: 1330942. https://doi.org/10.3389/fendo.2024.1330942.

[43] Kooman JP, Dekker MJ, Usvyat LA, Kotanko P, van der Sande FM, Schalkwijk CG, *et al*. Inflammation and premature aging in advanced chronic kidney disease. American Journal of Physiology. Renal Physiology. 2017; 313: F938–F950. https://doi.org/10.1152/ajprenal.00256.2017.

[44] Zhang K, Zhang Y, Feng W, Chen R, Chen J, Touyz RM, *et al*. Interleukin-18 Enhances Vascular Calcification and Osteogenic Differentiation of Vascular Smooth Muscle Cells Through TRPM7 Activation. Arteriosclerosis, Thrombosis, and Vascular Biology. 2017; 37: 1933–1943. https://doi.org/10.1161/ATVBAHA.117.309161.

[45] Zhang Y, Zhang K, Zhang Y, Zhou L, Huang H, Wang J. IL-18 Mediates Vascular Calcification Induced by High-Fat Diet in Rats With Chronic Renal Failure. Frontiers in Cardiovascular Medicine. 2021; 8: 724233. https://doi.org/10.3389/fcvm.2021.724233.

[46] Roumeliotis S, Roumeliotis A, Dounousi E, Eleftheriadis T, Liakopoulos V. Biomarkers of vascular calcification in serum. Advances in Clinical Chemistry. 2020; 98: 91–147. https://doi.org/10.1016/bs.acc.2020.02.004.